

*N114W-2373
11-74-CR
191207
29F*

Filters for the International Solar Terrestrial Physics (ISTP) mission far ultraviolet imager

Muamer Zukic, Douglas G. Torr, Jongmin Kim

Department of Physics
The University of Alabama in Huntsville
Optics Building, Suite 300
Huntsville, AL 35899
Phone: (205) 895-6238 x 374
Fax: (205) 895-6717

James F. Spann and Marsha R. Torr

NASA/Marshall Space Flight Center
Huntsville, AL 35812
Phone: (205) 544-7591
FAX: (205) 544-5862

(NASA-CR-194633) FILTERS FOR THE
INTERNATIONAL SOLAR TERRESTRIAL
PHYSICS (ISTP) MISSION FAR
ULTRAVIOLET IMAGER (Alabama Univ.)
29 p

N94-15868

Unclass

G3/74 0191267

ABSTRACT

The far ultraviolet (FUV) imager for the International Solar Terrestrial Physics (ISTP) mission is designed to image four features of the aurora: O I lines at 130.4 nm and 135.6 nm and the N₂ Lyman-Birge-Hopfield (LBH) bands between 140 nm - 160 nm (LBH long) and 160 nm -180 nm (LBH long). In this paper we report the design and fabrication of narrow-band and broadband filters for the ISTP FUV imager. Narrow-band filters designed and fabricated for the O I lines have a bandwidth of less than 5 nm and a peak transmittance of 23.9% and 38.3% at 130.4 nm and 135.6 nm, respectively. Broadband filters designed and fabricated for LBH bands have the transmittance close to 60%. Blocking of out-of-band wavelengths for all filters is better than $5 \times 10^{-3}\%$ with the transmittance at 121.6 nm of less than $10^{-6}\%$.

Keywords: optical filters, optical coatings, far ultraviolet

1. INTRODUCTION

Airglow emissions in the far ultraviolet can provide valuable information on auroral energy input and on the identity and the characteristic energy of precipitating particles. Photometric imaging of terrestrial auroral emissions, constitutes an important aspect of NASA's role in the ISTP mission.

The primary objectives for the far Ultraviolet Imager (UVI) are to acquire coherent global images of the earth's aurora at two FUV emission lines (130.4 nm and 135.6 nm) and two emission bands (140-160 nm and 160-180 nm), from altitudes between six and nine earth's radii (R_E), with adequate spectral filtering

to allow the total energy flux and energy characteristics of precipitating particles to be retrieved. The UVI with 0.6 milliradians angular resolution over an 8° field of view sampled with 39,500 pixels, will provide coherent global auroral images with unprecedented filtering and spatial resolution performance.

The FUV imager consists of three aspherical mirrors with the center of the object field displaced 6° from the optical axis. This optical design was the first of a kind to provide both low focal ratio (f/2.9) and good spatial resolution over 8° field of view in the FUV. The design provides for an unobscured optical aperture, excellent baffling, flat field, provision for filter insertion and general compactness¹.

The overall performance of the instrument depends critically on the filter performance realized. In order to provide scientifically valuable data the imager must have two narrow-band filters with bandwidths of less than 5 nm, blocking for out-of-band wavelengths better than $3 \times 10^{-3}\%$, with transmittance at 121.6 nm of less than $10^{-6}\%$ and a peak transmittance of more than 20%. The broadband filters should have the same blocking for out-of-band wavelengths, 10-12 nm bandwidths and in-band transmittance greater than 50%.

Prior to the development effort undertaken for the UVI, filters with required spectral performance were nonexistent. The magnitude of the challenge can be evaluated when it is recognized that with exception of the bright H Ly α and OI 130.4 nm features, no far ultraviolet images had been previously achieved on the fully sunlit side of the earth, because of visible light leakage. The filtering requirements to extract the total energy flux and energy characteristics of precipitating auroral electrons are the following: 1) Measurement of N₂ Lyman-

Birge-Hopfield (LBH) bands from 160 - 180 nm (LBH long), and from 140 - 160 nm (LBH short) with better than 90% spectral purity, and 2) Measurement of OI emissions at 130.4 nm and 135.6 nm with spectral purity of more than 90%.

Narrow-band filters that were commercially available in the FUV wavelength region from 120 nm to 160 nm had a typical transmittance lower than 15% and full width measured at half of the transmittance maximum (FWHM) greater than 25 nm. The peak transmittance of the filters centered at the longer wavelengths from 160 nm - 230 nm were between 20% and 25% with FWHM \geq 20 nm.

Malherbe² reported the design and the spectral performance of a narrow-band filter centered at the Lyman- α (121.6 nm) with peak transmittance close to 15% and FWHM = 9 nm. Blocking of the wavelengths longer than 160 nm is better than 10⁻³%. The filter has relatively high transmittance for the wavelength region from 126 nm - 135 nm; close to 7% at 126 nm and almost 1% at 135 nm. This pass window renders the filter not very useful for terrestrial imaging applications if spectral discrimination of the neighboring atomic oxygen lines at 130.4 nm and 135.6 nm is desired. A narrow-band filter centered at 202.5 nm is reported by the same author³. The filter has peak transmittance greater than 85% and FWHM = 2.5 nm. However, the blocking zone of the filter is very short and the transmittance for wavelengths longer than 220 nm becomes greater than 85%.

The calculated and experimental spectral performance of a Fabry-Perot-type narrow-band filter centered at 179 nm was reported by Spiller⁴. His theoretical calculations predicted a narrow-band filter with resolution $\lambda_0/\Delta\lambda = 60$

and a peak transmittance of 25%, but the measured performance had almost a four times smaller resolution and a much smaller peak transmittance. Discrepancies between the theoretically predicted and experimentally obtained spectral curves have been ascribed to the excitation of a surface plasma wave traveling along the surface of an aluminum film.

A variable bandwidth transmission filter reported by Elias⁵ had bandwidths from 7 nm to 20 nm with a peak transmittance from 20% to 40%, respectively. The filter was centered at 176 nm, and as in the case of other all-dielectric transmission filters, suffered from pass windows in the longer wavelength region. Narrow-band filters for the FUV wavelength range from 120 nm to 230 nm with similar optical properties to those listed above were also reported by some other authors⁶⁻⁹. Broadband filters with bandwidths greater than 10 nm, which are currently available in the FUV have a relatively low transmittance, poor out-of-band rejection, and most of them have the shape of a transmittance spectral curve similar to that of the Fabry-Perot-type filters²⁻⁹.

Taking all this into account, it becomes obvious that the FUV spectral range lacked high quality narrow- and broadband filters which would satisfy the filtering requirements of the ISTP imager . Certainly a lack of low absorbing film materials in the FUV wavelength range for the all-dielectric filters and the coupling of the incident light into plasma surface waves of the metal for metal-dielectric filters were reasons for this.

Hunter¹⁰ achieved a measure of success in solving this problem by combining two or more reflectors in a series to achieve the desired spectral performance for the design of the FUV reflection polarizers and analyzers. The

idea is that, if sufficiently high reflectivity can be achieved within the passband, the in-band exponential loss of reflectivity with additional reflective surfaces becomes insignificant compared with the net out-of-band exponential loss. However for the approach to be viable, the ratio of in-band to out-of-band reflectivity at each surface should be of the order of 30, e.g., 90% and 3%, respectively. Three reflections, for example, then reduce the in-band reflectivity to 72.9%, whereas the out-of-band reflectivity is reduced to $2.7 \times 10^{-3}\%$ and so on.

In this paper we report the successful design and fabrication of high-reflectance narrow-band and broadband reflection filters. These filters are then combined into a multiple reflector to provide excellent blocking for out-of-band wavelengths and the desired spectral shape for both narrow-band and broadband applications. The blocking for shorter out-of-band wavelengths is improved by means of additional transmission filters. The filter combinations provided better than originally specified spectral performance of the ISTP far ultraviolet imager.

2. FUV THIN FILM AND SUBSTRATE MATERIALS

The first step in the development of our technology for the design and fabrication of FUV filters is the determination of optical constants (refractive index and extinction coefficient) of film materials within the FUV range. Our laboratory has recently developed the experimental and theoretical techniques for the determination of the optical constants of films and substrates in the FUV¹¹. An iterative approach implemented into the thin film design program¹² is used to derive optical constants from photometric measurements^{13,14}.

On the basis of the measurements conducted to date, it would appear that only the following bulk materials have useful optical properties for FUV applications: MgF₂ was the only material identified as suitable as a substrate for transmission filters for wavelength range below 140 nm; BaF₂, and SiO₂ can be used as substrate materials for wavelengths above 140 nm and 160 nm, respectively; Pyrex because of the low cost, excellent mechanical and chemical resistance, and its susceptibility to a very high quality polishing was found to be the best substrate for reflection filters. Suitable film materials include BaF₂, CaF₂, LaF₃, MgF₂, Al₂O₃, and SiO₂. With the knowledge acquired of the optical constants for these materials, it now becomes possible to design coatings suitable for such FUV devices as narrow-band and broadband filters¹¹⁻¹⁹.

3. NARROW-BAND REFLECTION FILTERS

In order to explain FUV narrowband filters, we start from a Π -multilayer design concept^{16,17}. For the quarterwave (QW) periodic multilayer case where two film materials have optical thicknesses corresponding to a quarter of a wavelength, it is known that the maximum reflectance of a periodic stack is given by²⁰

$$R_k = 1 - 2\pi n_0 \frac{k_H + k_L}{n_H^2 - n_L^2} \quad (1)$$

where n_H and n_L are refractive indices of high and low index film materials, and k_H and k_L are corresponding extinction coefficients.

The ultimate reflectance, R_k , is usually referred to as the Koppelman limit. It should be emphasized that Eq. (1) is derived with some approximations and cannot replace an exact calculation of the maximum reflectance of a periodic stack. Furthermore, for wavelength regions in which the refractive index is less than one, the Koppelman formula does not give the correct answer for the ultimate reflectance.

The principle of the Π -stack approach is to use a combination of high (H) and low (L) refractive index dielectric pairs so that $H + L = \lambda/2$, where $L/H > 1$, and H and L designate the optical thicknesses of high- and low-index film materials. Since the phase thicknesses of an HL pair add to Π , we call stacks made of such pairs Π -stacks or Π -multilayers. Thus, a quarterwave stack (QW; optical thicknesses of layers are $\lambda/4$) is a special case of Π -multilayers with the ratio $L/H = 1$.

In a QW stack the light that is reflected from all interfaces is in phase, while in a Π multilayer the light that is reflected from each HL pair is in phase. Obviously, QW stacks with low-absorbing film materials (which are available in visible and infrared parts of the spectrum) provide higher reflectance with fewer layers than other Π -stacks. However, in the FUV and EUV where low-absorbing high-index film materials do not exist, a Π -multilayer with a smaller physical thickness of H relative to L provides lower absorptance and therefore higher reflectance of the stack¹⁶⁻¹⁹.

Figure 1 shows maximum reflectance as a function of the L/H ratio of a 35-layer reflection filter designed for 145 nm and 45° angle of incidence using MgF₂ and LaF₃. The reflector has a maximum reflectance when the ratio $L/H =$

3. This corresponds to the optical thickness of $L(\text{MgF}_2) = 3\lambda/8$ and $H(\text{LaF}_3) = \lambda/8$. The Koppelman limit (QW stack; $L/H = 1$) for this design is 89.6%.

As the optical thickness ratio (L/H) of the Π -multilayer changes, the high reflectance bandwidth, or so-called full width at half of the reflectance maximum, (FWHM) also changes. This property is used to control the high reflectance bandwidth of the filter. Figure 2 shows the bandwidth of the 35-layer stack designed for 145 nm and 45° angle of incidence using MgF_2 (L) and LaF_3 (H) as a function of L/H ratio.

It is obvious that for the design of a narrowband reflector ratio, L/H has to be as high as possible. However, an increase of the L/H ratio requires the addition of more layers to the stack in order to maintain reflectance at its design maximum. Furthermore, the value of the L/H ratio and therefore the minimum thickness of an H layer is certainly limited by the feasibility of depositing and monitoring extremely thin layers. Other important factors that limit the maximum value of the L/H ratio include substrate surface roughness and structural properties of the layers.

Figure 3 shows the measured net transmittance through three 130.4 nm Π multilayer narrowband reflection filters combined with a transmission filter. A transmission filter and three reflection filters are mounted in the filter box. The reflection filters are 35-layer Π -stacks with optical thicknesses $H = \lambda/8$, and $L = 3\lambda/8$ designed for 130.4 nm and 45° angle of incidence using MgF_2 as the low (L) and LaF_3 as the high refractive index material (H). The transmission filter is $\text{BaF}_2/\text{MgF}_2$ 2-layer absorbing stack deposited on a MgF_2 substrate. The peak transmittance of the combination is greater than 23% with 4.5 nm bandwidth.

The average blocking for out-of-band wavelengths up to 2500 nm is better than $3 \times 10^{-3}\%$ with less than $10^{-6}\%$ transmittance at 121.6 nm (see Figure 7).

Figure 4 shows the measured net transmittance through three narrowband reflection filters centered at 135.6 nm combined with a cut-on transmission filter. The reflection filters are 35-layer Π stacks with optical thicknesses $H = \lambda/8$, and $L = 3\lambda/8$, where MgF_2 is the high and LaF_3 is the low refractive index material. The filters are designed for 135.6 nm and 45° angle of incidence using. The transmission filter is a $\text{BaF}_2/\text{MgF}_2$ 2-layer absorbing stack deposited on a MgF_2 substrate. The peak transmittance of the filter combination is greater than 38% with less than 5 nm bandwidth. The average transmittance for out-of-band wavelengths ($\lambda < 2500$ nm) is less than $3 \times 10^{-3}\%$, and less than $10^{-6}\%$ at 121.6 nm (see Figure 7).

4. BROADBAND REFLECTION FILTERS

The pass zone of a broadband filter is bounded by lower and upper wavelengths. Ideally, the spectral components of the incident light with wavelengths shorter than the lower and longer than the upper wavelength of the filter, together referred to as the out-of-band spectrum, are rejected. In the design examples that follow, wavelengths of the out-of-band spectrum are rejected by means of multiple reflections from QW stacks.

The rejection at shorter wavelengths might be improved by the suitable choice of the window material, placed at the entrance of a multi-reflector combination. Windows made of BaF_2 and CaF_2 absorb wavelengths below 135

nm, and 125 nm respectively, while Fused Silica and aluminum oxide may be used for broadband filters with a lower pass limit above 145 nm¹¹.

Due to the narrower high reflection zone, the Π multilayers with $L/H > 1$ are not suitable for the design of broadband reflectors (see Fig. 2). A QW stack for which $L/H = 1$ is a better choice for the design and fabrication of these filters. Figure 5 shows the measured net transmittance through the combination of three 35-layer QW-stacks ($L/H=1$) as reflection filters designed for LBH short FUV bands, with a BaF₂ substrate with protective MgF₂ coating as the transmission filter. The reflection filters are designed for 150 nm and 45° angle of incidence using MgF₂ as the low (L) and LaF₃ as the high refractive index material (H). The filter combination has a peak transmittance of more than 60% and a bandwidth of 11 nm.

Figure 6 shows the measured net transmittance through the filter combination designed for the LBH long FUV bands. The combination comprises three 35-layer Π -stacks as reflection filters, and a bare fused silica substrate as the transmission filter. The reflection filters are centered at 170 nm and designed for 45° angle of incidence using MgF₂ as the low (L) and LaF₃ as the high refractive index material (H).

The filter combination shown in Figure 6 has a peak transmittance close to 60% and a bandwidth of 11 nm. The average rejection of the out-of-band spectrum up to 2500 nm is better than $3 \times 10^{-3}\%$ with the transmittance for wavelengths below 150 nm of less than $10^{-6}\%$.

5. COATING AND TESTING LAB

All thin film depositions during the research for the ISTP program were made at the University of Alabama in Huntsville, Optical Aeronomy Laboratory, and spectrophotometric measurements were made at the Space Science Laboratory of the NASA/Marshall Space Flight Center. The high vacuum system comprising an e-beam coater consists of a cryo-pump and absorption pump giving an oil-free environment for all depositions and therefore a very low probability of hydrocarbon contamination of the films. A quartz crystal monitor is used for the film thickness and deposition rate monitoring.

The filter substrates were cleaned by the supplier (Acton Research Corp., Acton, MA) using the following procedure: optical soap wash, water rinse, ethanol soak then ultrasonic bath, fresh ethanol rinse, and finally Freon rinse. The elliptically shaped Pyrex reflection filter substrates range in size from approximately 6 x 4 cm to 8 x 6 cm. The transmission filter substrates made of fused silica, MgF₂, and BaF₂ had 5 cm diameter. All substrates were shipped in dry nitrogen purged delrin holders and were only removed immediately prior to deposition.

The depositions were made with a fixed voltage (10 kV) electron beam gun on heated substrates. The films were deposited with deposition rates ranging from 0.14-0.25 nm/sec at pressures below 10⁻⁵ Torr. The temperature of the substrate was monitored with a Chromel-Alumel thermocouple attached to aluminum substrate holder. The filter substrate temperature was kept at 175°C during deposition. The substrate and its ring holder were placed on 6 mm thick stainless steel plate with 50 cm diameter. The source-to-substrate distance was 50

cm and source-to-oscillator (thickness monitor) distance was 35 cm. After deposition, the substrates were allowed to cool to 30°C, and the vacuum chamber was vented with dry nitrogen.

Deposited substrates were kept in a clean room environment (class better than 10 particles(5-0.5 μ m/cft.). Although the filters were exposed to the environment (10 - 20 months) in which only temperature and particle contamination were controlled the degradation of the spectral performance has never been detected. Both reflection and transmission filters did not exhibit any change in the spectral performance after exposure to the simulated high energy radiation of space environment²¹.

Transmittance and reflectance measurements were performed in a hydrocarbon-free vacuum system at pressure below 10⁻⁵ Torr. A sealed deuterium lamp with a MgF₂ window was used in tandem with 0.2 m monochromator producing a beam with 1 nm spectral resolution. Folding and collimating optics were used to produce a 1 x 0.74 cm reference beam. An FUV detector consists of a sodium salycilate coated Pyrex window placed in front of a bialkali photometer¹¹.

6. SUMMARY

The FUV filters designed and fabricated for the ISTP program were made as combinations of three reflection and one transmission filter. Narrow-band filtering with a bandwidth of 5 nm and a throughput at the central wavelength of more than 20% and 35% is achieved at 130.4 and 135.6 nm, respectively, with the average blocking of out-of-band wavelengths of better than 3x10⁻³%. In the

case of broadband filters a multiple reflector centered at 150 and 170 nm combined with corresponding transmission filters had a bandwidth close to 11 nm and the transmittance greater than 60% for both LBH bands. The average blocking of out-of-band wavelengths is better than $3 \times 10^{-3}\%$.

The idea of utilizing the multiple reflections from Π multilayer reflectors constitutes the basis of the ISTP FUV narrow-band and broadband filters. The multiple reflector combinations provide spectral performance for narrow and broadband filters superior to what is currently available with an in-band to out-of-band ratio of more than 10^4 which provides measurements of four key FUV features with spectral purity of 98% for 130.4 nm, 90% for 135.6 nm, 99% for LBH short and 99% for LBH long. Together with a solar blind intensified CCD detector, a net rejection of better than 10^{-9} of all FUV and visible out-of-band emissions is achieved.

The substantial advances in the area of the FUV coating technology greatly enhance what can now be achieved in terms of FUV filtering and imaging. The ability to quantitatively separate spectral features means that where previously, 60% to 80%, or more, of the measured signal was contaminant, now 90% to 99% of the signal is the spectral feature of interest. The ISTP Ultraviolet Imager with its superior filtering and imaging characteristics will provide about two orders of magnitude improvement in performance over previous designs.

7. ACKNOWLEDGMENTS

This work was supported by NASA contract NAS8-38145 and NASA grant NAGW-2898. We are indebted to Dr. Charles Keffer for his assistance in

measuring the reflectance and transmittance of the filters. The third author, J. Kim, would like to thank the Physics Department of the University of Alabama in Huntsville for the graduate student assistantship received during this study, and the Agency for Defense Development of Korea for additional financial support.

8. REFERENCES

1. D. G. Torr, M. R. Torr, M. Zukic, J. Spann, and R. B. Johnson, "The ultraviolet imager (UVI) for ISTP", *Proc. SPIE*, **1745**, 61-74 (1992), and *Opt. Eng.* this volume.
2. A. Malherbe, "Interference filters for the far ultraviolet", *Appl. Opt.*, **13**, 1275-1276 (1974).
3. A. Malherbe, "Multidielectric components for the far ultraviolet", *Appl. Opt.*, **13**, 1276-1276 (1974).
4. E. Spiller, "Multilayer interference coatings for the vacuum ultraviolet" in *Space Optics*, B. J. Thompson and R. R. Shanon eds. *Proc. of the Ninth International Congress of the International Commission for Optics*, 581-597 (National Academy of Sciences, Washington, D.C., 1974).
5. L. R. Elias, R. Flach, and W. M. Yen, "Variable bandwidth transmission filter for the vacuum ultraviolet: $\text{La}_{1-x}\text{Ce}_x\text{F}_3$ ", 2239-2240, *Appl. Opt.* **12**, 138-139 (1973).

6. E. T. Fairchild, "Interference filters for the VUV (1200-1900 Å)", *Appl. Opt.*, **12**, 2240-2241 (1973).
7. B. K. Flint, "Special application coatings for the vacuum ultraviolet (VUV)", *Opt. Eng.*, **18**, 92-97 (1979).
8. B. K. Flint, "Special application coatings for the vacuum ultraviolet", *Proc. SPIE*, **140**, 131-139 (1978).
9. W. R. Hunter, "Review of vacuum ultraviolet optics", *Proc. SPIE*, **140**, 122-131 (1978).
10. W. R. Hunter, "Design criteria for reflection polarizers and analyzers in the vacuum ultraviolet", *Appl. Opt.*, **17**, 1259-1270, (1978).
11. M. Zukic, D. G. Torr, J. F. Spann, and M. R. Torr, "Vacuum ultraviolet thin films. 1: Optical constants of BaF₂, CaF₂, LaF₃, MgF₂, Al₂O₃, HfO₂, and SiO₂ thin films", *Appl. Opt.*, **29**, 4284-4292 (1990).
12. M. Zukic, "Damped least squares technique for the design of optical multilayer filters", M. S. Thesis, Imperial College, London (1984).
13. M. Zukic, "Optical filters in the vacuum ultraviolet", PhD Dissertation, the University of Alabama in Huntsville (1989).

14. M. Zukic, and D. G. Torr, "VUV thin films", in *Topics in Applied Physics*, K. H. Guenther ed., Chapter VII, Springer-Verlag series on Thin Films, in press.
15. M. Zukic, D. G. Torr, J. F. Spann, and M. R. Torr, "Vacuum ultraviolet thin films 2: Vacuum ultraviolet all-dielectric narrow-band filters", *Appl. Opt.*, **29**, 4293-4302 (1990).
16. M. Zukic, and D. G. Torr, "Multiple reflectors as narrow-band and broadband VUV filters", *Appl. Opt.*, **31**, 1588-1596 (1992).
17. M. Zukic, D. G. Torr, and J. Kim, "X-ray, extreme and far ultraviolet optical coatings for space applications", in *Trends in Optical Engineering*, edited by Council of Scientific Research Integration, to be published by Research Trends, in press.
18. M. Zukic, and D. G. Torr, "High-throughput narrowband 83.4 nm self-filtering camera", *Proc SPIE* **1546**, 234-244 (1991).
19. M. Zukic D. G. Torr, and J Kim, "Extreme ultraviolet filters for 58.4 and 83.4 nm", *Proc. SPIE* **1744**, 178-187 (1992).
20. G. Koppelman, "On the theory of multilayers consisting of weakly absorbing materials and their use as interferometer mirrors", *Ann. Phys. Leipzig* **5**, 388-396 (1960).

21. C. E. Keffer, M. R. Torr, M. Zukic, J. Spann, D. G. Torr, and J. Kim, "Radiation damage effects in far ultraviolet filters and substrates", *Appl. Opt.*, in press.

FIGURE CAPTIONS

Figure 1. Change in the calculated reflectance of a 35-layer Π -multilayer as the optical thickness ratio(L/H) changes, where MgF₂ is used as the low (L) and LaF₃ as the high (H) refractive index material. The Koppelman limit for this case is 89.6%.

Figure 2. Full width at half of the reflectance maximum of 35-layer Π -stacks calculated for a 45° angle of incidence at 135.5 nm, where H represents optical thickness of a LaF₃, and L optical thickness of MgF₂ film.

Figure 3. The measured net transmittance (solid line) through three narrowband reflection filters (dashed line) centered at 130.4 nm, and combined with the transmission filter (dotted line). The reflection filters operate at 45° angle of incidence. MgF₂ and LaF₃ are used as the low and high refractive index materials, respectively. The peak transmittance is greater than 22%, with 5 nm bandwidth. The average blocking for out-of-band wavelengths up to 2500 nm is better than $3 \times 10^{-3}\%$ with transmittance less than $10^{-6}\%$ at 121.6 nm (see Fig. 7).

Figure 4. The measured net transmittance (solid line) through three narrowband reflection filters (dashed line) centered at 135 nm, and combined with the transmission filter (dotted line). The reflection filters which are designed using MgF₂ as the low and LaF₃ as the high refractive index material operate at 45° angle of incidence. The peak transmittance is greater than 38%, with 4.5 nm bandwidth. The average blocking for out-of-band wavelengths up to 2500 nm is better than $3 \times 10^{-3}\%$ with transmittance less than $10^{-6}\%$ at 121.6 nm (see Fig. 7).

FIGURE CAPTIONS (Continued)

Figure 5. The measured net transmittance (solid line) through three broadband reflection filters (dashed line) centered at 150 nm, and combined with the transmission filter (dotted line). The reflection filters operate at 45° angle of incidence. They are designed using MgF₂ as the low and LaF₃ as the high refractive index material. The peak transmittance is close to 60%, with 10 nm bandwidth. The average blocking for out-of-band wavelengths up to 2500 nm is better than $3 \times 10^{-3}\%$ with less than $5 \times 10^{-6}\%$ transmittance for wavelengths below 145 nm (see Fig. 7).

Figure 6. The measured net transmittance (solid line) through three broadband reflection filters (dashed line) centered at 170 nm, and combined with the transmission filter (dotted line). The reflection filters operate at 45° angle of incidence. They are designed using MgF₂ as the low and LaF₃ as the high refractive index material. The peak transmittance is close to 60%, with 11 nm bandwidth. The average blocking for out-of-band wavelengths up to 2500 nm is better than $3 \times 10^{-3}\%$ with less than $5 \times 10^{-6}\%$ transmittance for wavelengths below 130 nm (see Fig. 7).

Figure 7. The total response of the Ultraviolet Imager filters (log. scale). Circles (○) represent response of OI line filter at 130.4 nm, squares (◻) response of OI line filter at 135.6 nm, diamonds (◊) response of LBH short band filter, and triangles (Δ) represent response of the filter for LBH long band.

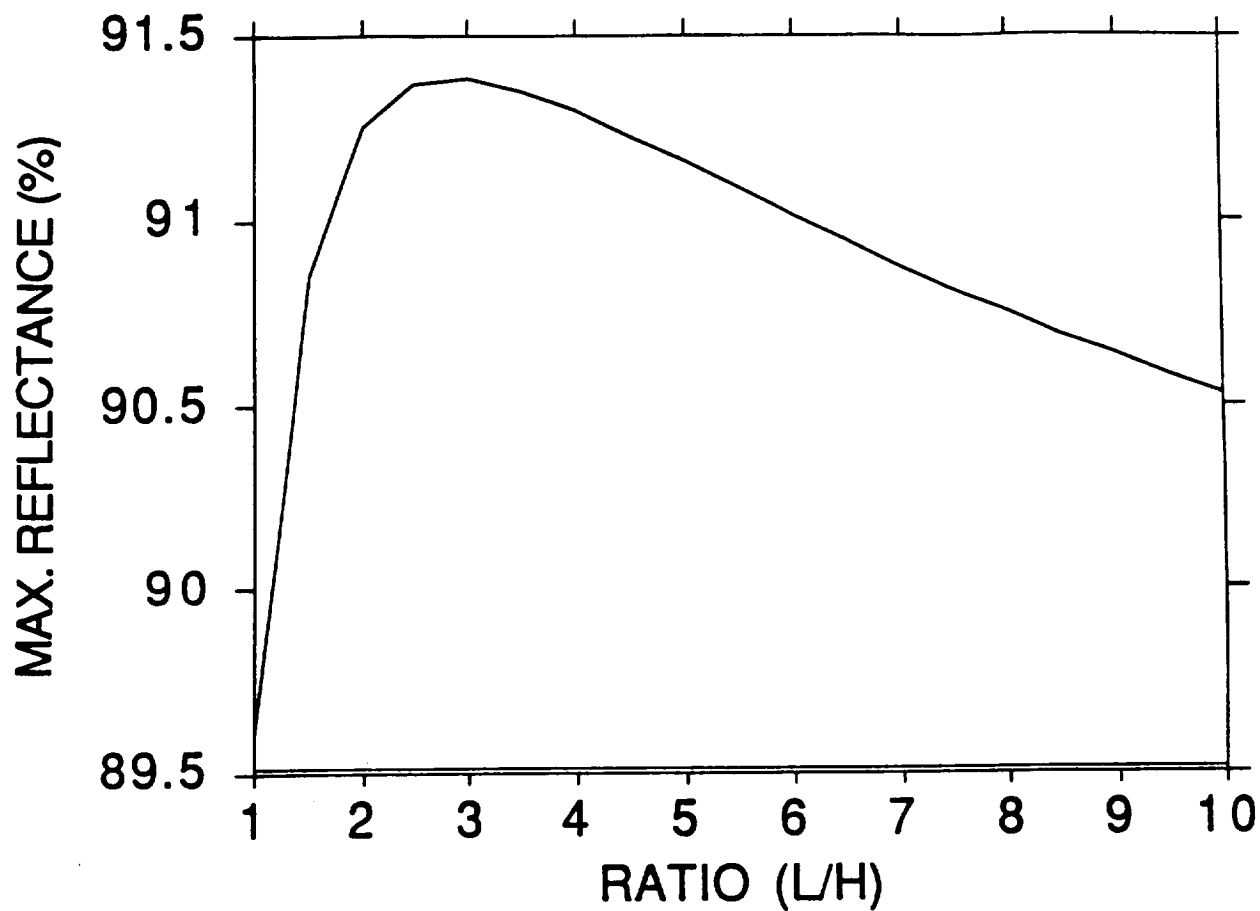


Figure 1.

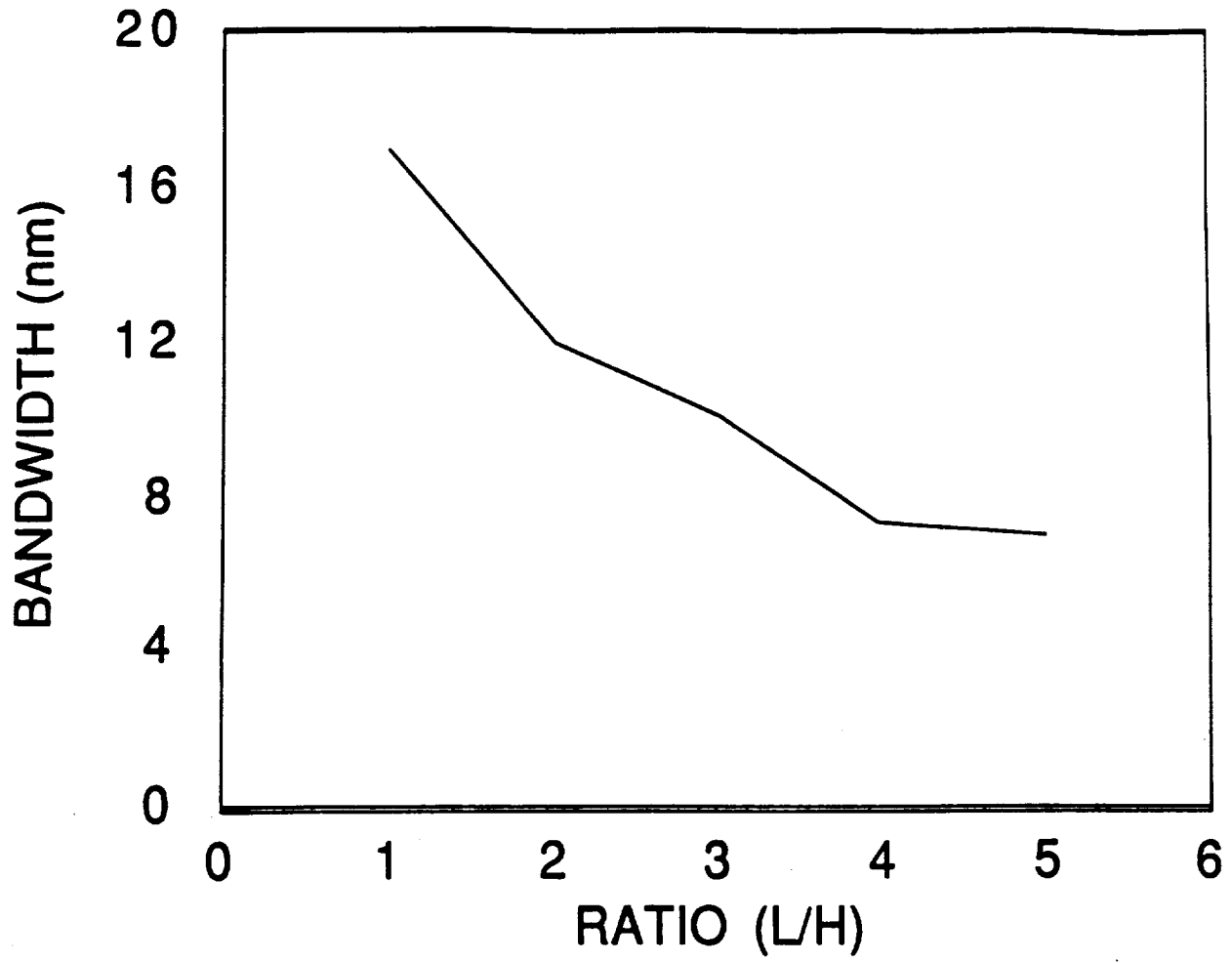


Figure 2.

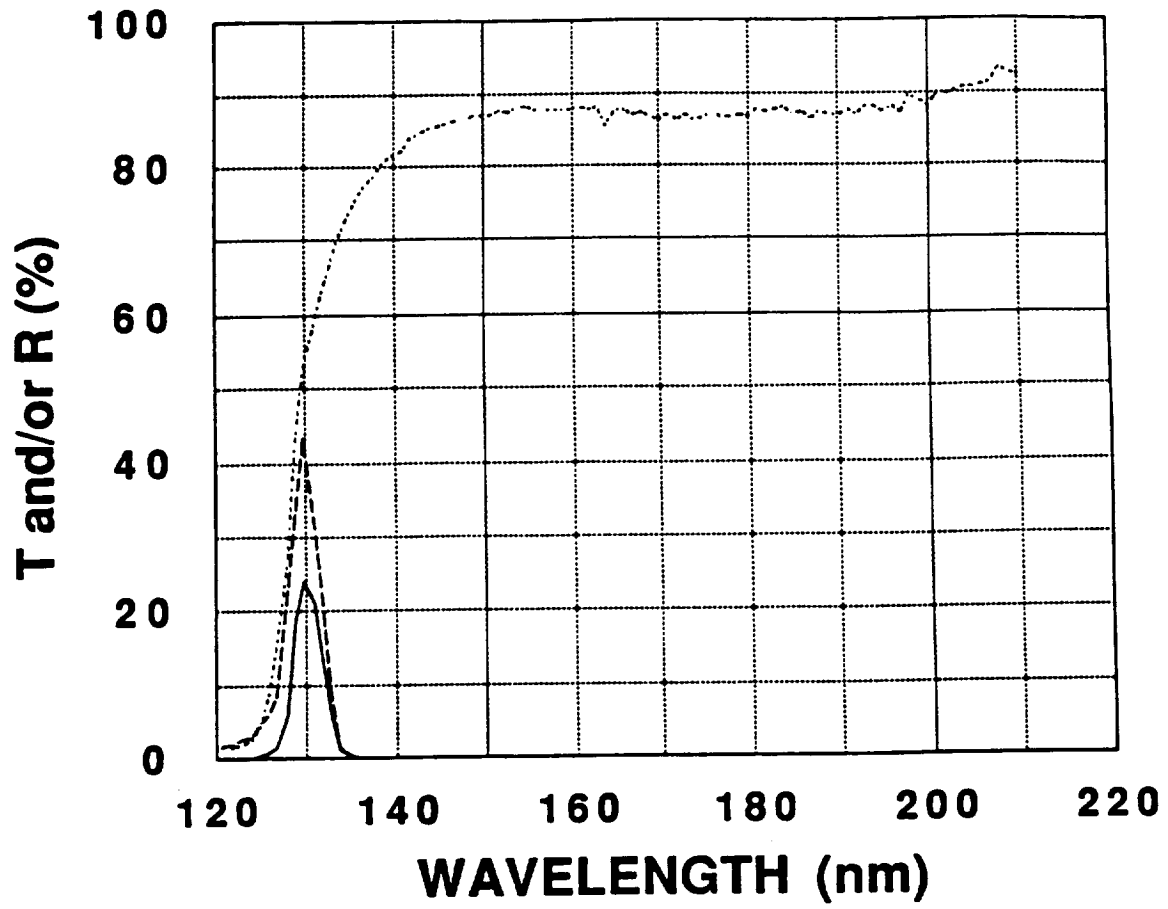


Figure 3.

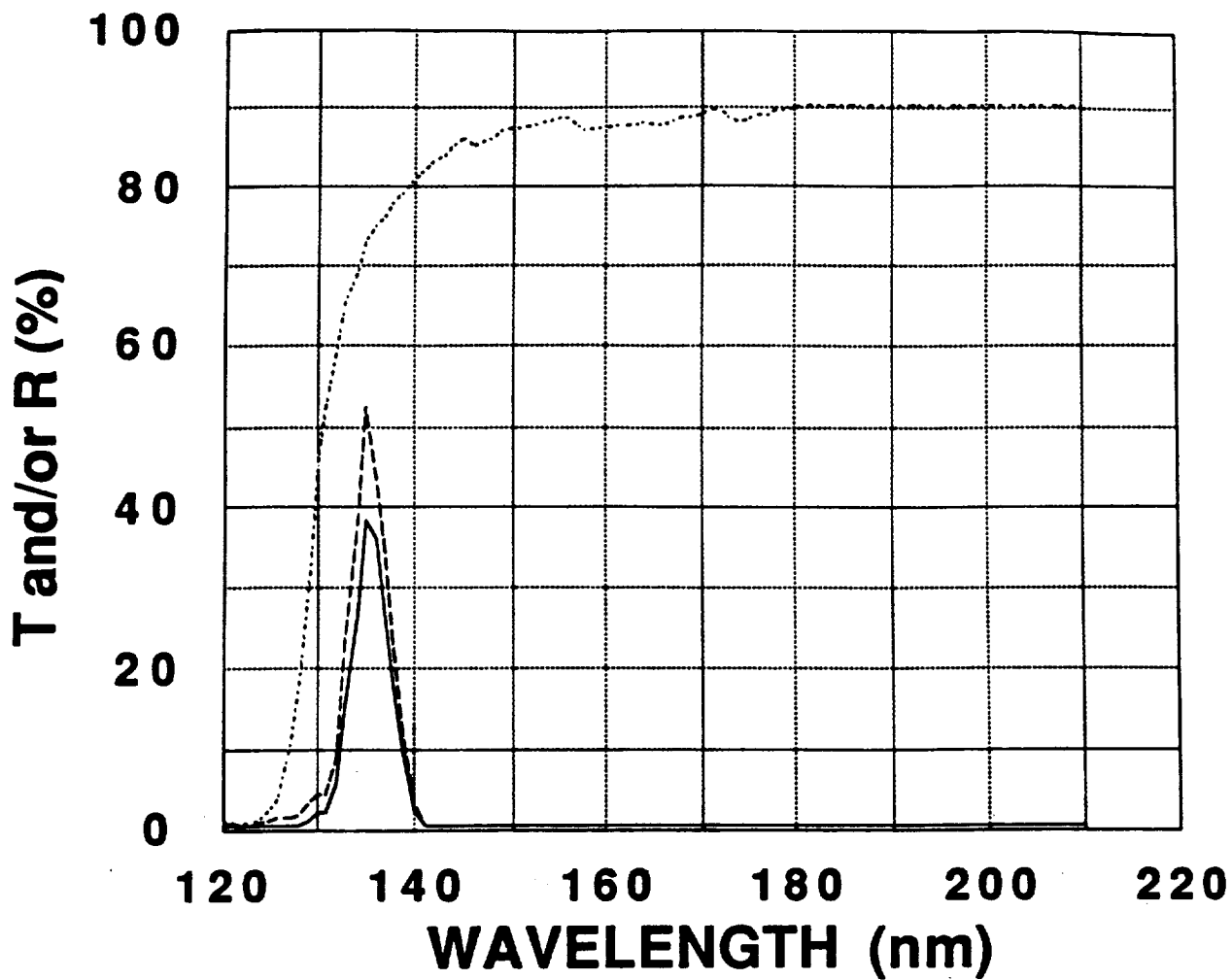


Figure 4.

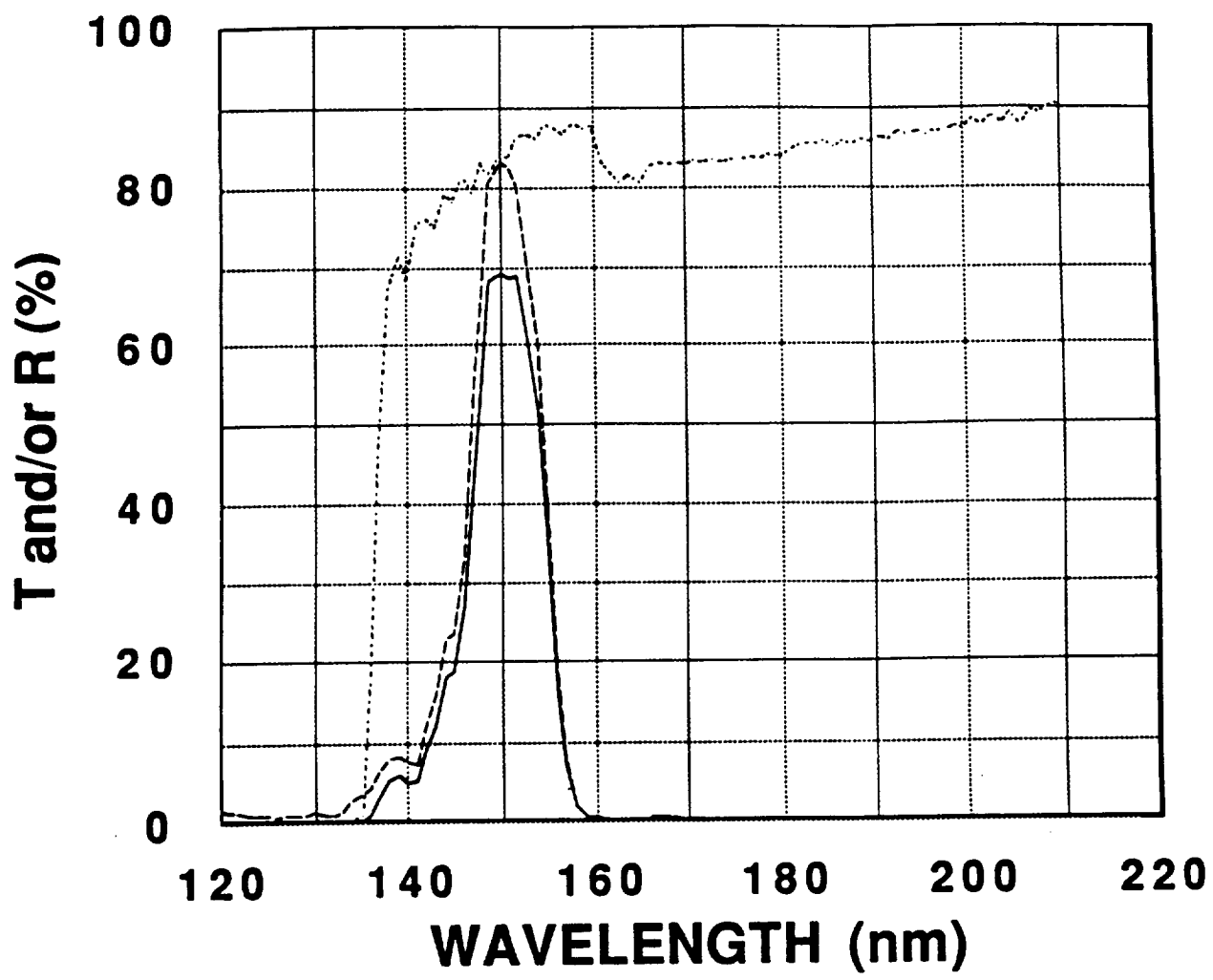


Figure 5.

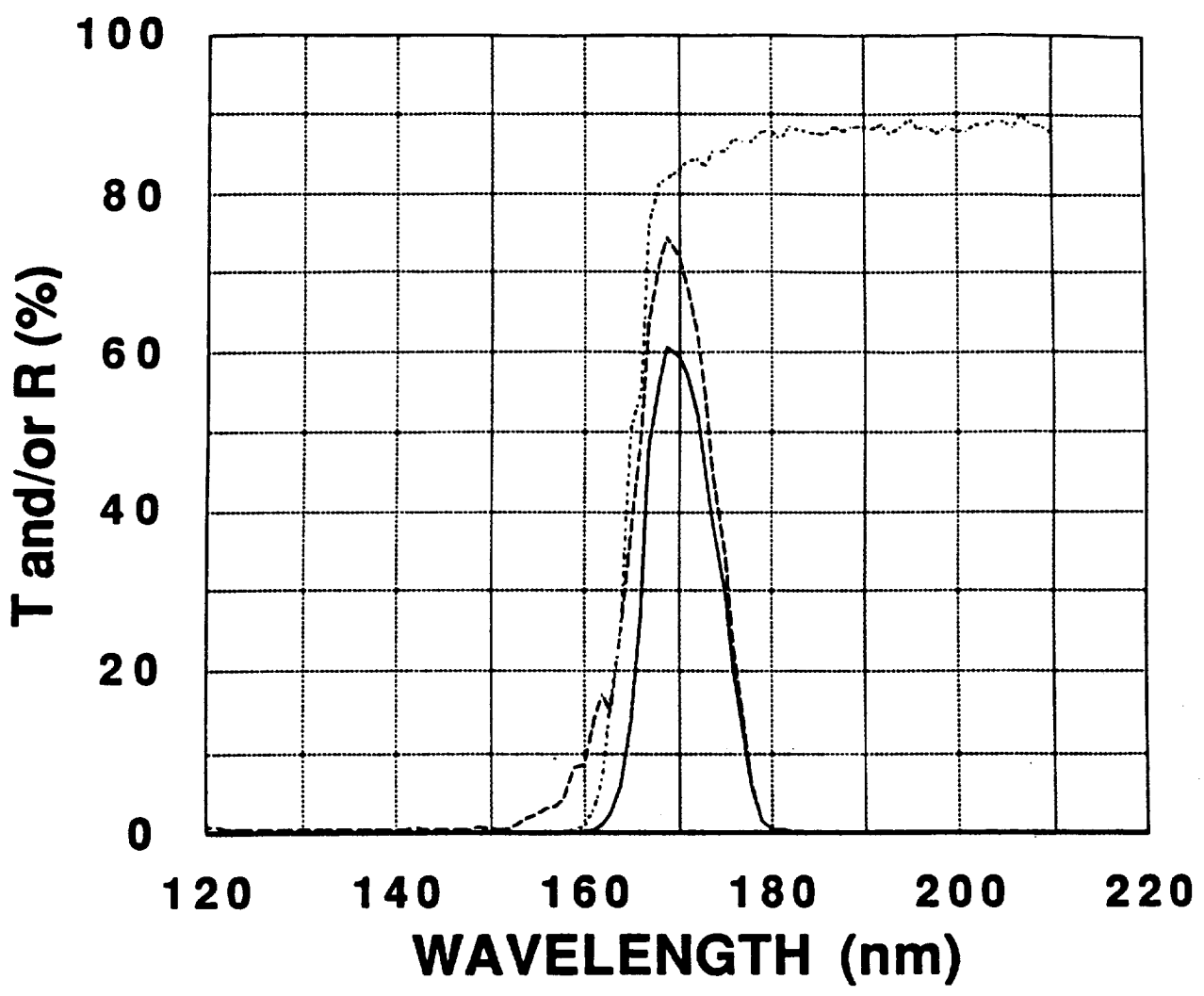


Figure 6.

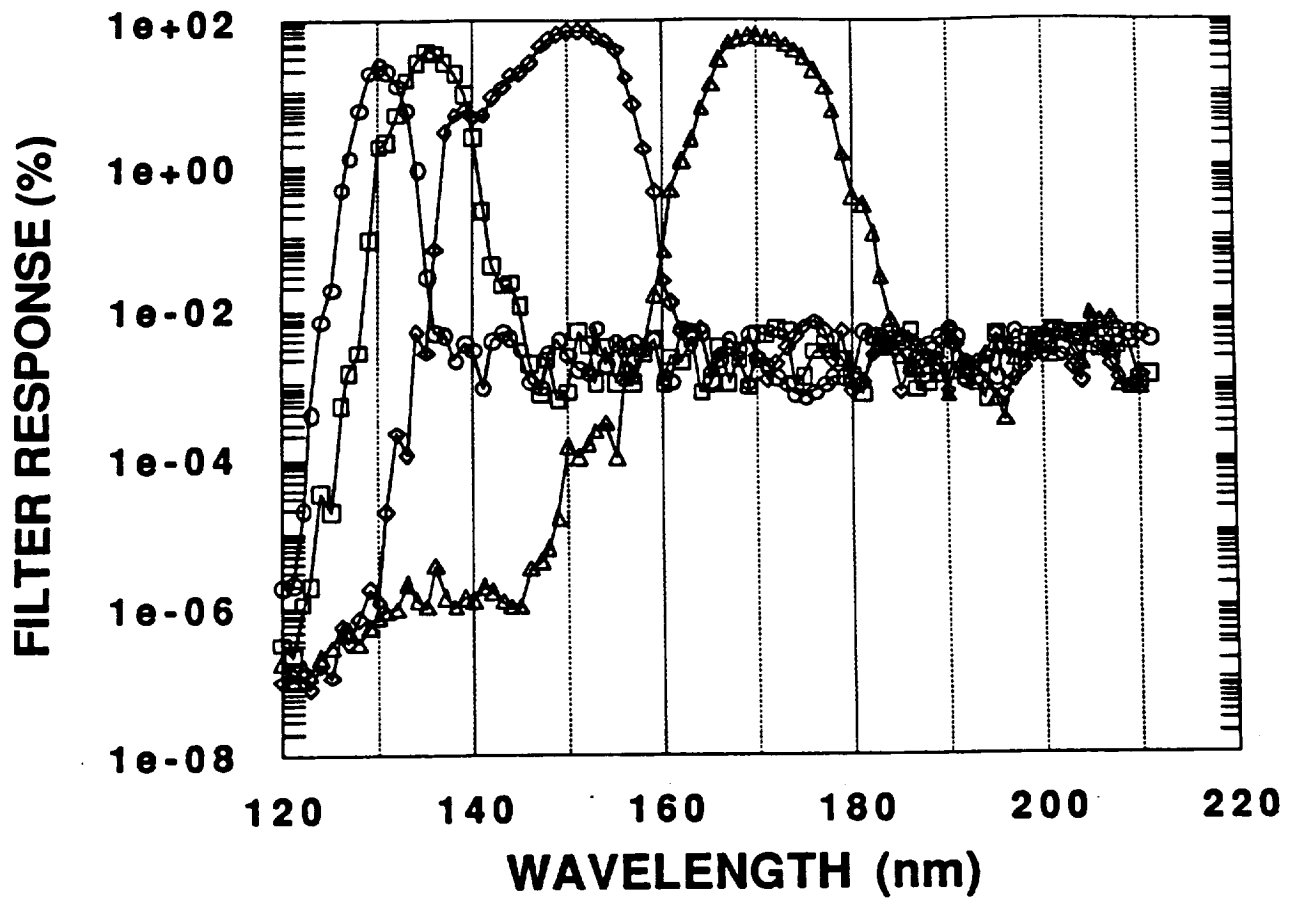


Figure 7.

Muamer Zukic received his B.S. degree in physics from the University of Sarajevo in 1979, M.S. degree in applied optics from Imperial College in London in 1984, and Ph.D. degree in physics from the University of Alabama in Huntsville (UAH) in 1989. As a graduate student he received a Newport Research Committee award and the "Academic Honor" award from the UAH. He has authored and co-authored more than 25 papers in refereed journals and conference proceedings, and contributed chapters in three books on optical thin films, and optical engineering. Dr. Zukic is presently a Senior Research Scientist in the Physics Department at the UAH. His research interest includes design and fabrication of optical thin films, optical characterization of solids and thin films, gradient index films., optical testing, lens design, space environmental effects on solids and films, remote sensing instrumentation development, and detector technology.

Douglas G. Torr received his BS in physics and chemistry from Rhodes University in 1961, and Ph.D. in physics in 1967. During his 25 years of research in aeronomy Dr. Torr has published 189 papers in refereed journals and presented more than 209 papers at professional meetings. He served as Co-Investigator on the Atmosphere Explorer Team, the Imaging Spectrometric Observatory (ISO) for Spacelab 1, the Ultraviolet Imager for ISTP and is P.I. on the ISO to be flown on the Atmospheric Laboratory for Applications and Science.

Jongmin Kim received the BS degree in 1977 from Korea University in Seoul Korea. After working in the Agency for Defense Development of Korea for eleven years he came to the University of Alabama in Huntsville (UAH) to continue his study. He received the MS degree in 1990 from the Physics

Department of the UAH and is pursuing his Ph.D. degree. His current research interest includes extreme and far ultraviolet coatings, optical properties of film and bulk materials in FUV and EUV regions, and effects of space environment on film and bulk materials.

James F. Spann received his Ph.D. degree in 1984 from the University of Arkansas in Fayetteville. From 1984-1986, he was an Oak Ridge Associated Universities Post Doctoral Fellow at the US Department of Energy in Morgantown, West Virginia. In 1986, Dr. Spann joined NASA/Marshall Space Flight Center, Huntsville, Alabama. His research interests include design and fabrication of space flight optical instruments, optical characterization of solid and thin films, the interaction of single particles with light and the equilibrium phases of atmospheric aerosols.

Marsha R. Torr received her MS and Ph.D. degrees from Rhodes University, South Africa. Dr. Torr is currently chief scientist in the project payloads office of the Marshall Space Flight Center, Principal Investigator on the UVI for ISTP, and Mission Scientist for the ATLAS-1 mission. During her scientific career, Dr. Torr has published over 110 papers in refereed literature, has advanced the technology in space optics and focal plane array detectors, has served on national and international committees, and has held various offices of the American Geophysics Union.

